Structure and Properties of Consolidated Amorphous Metal Powder

F. S. Biancaniello[1], T. F. Zahrah[2], R. D. Jiggetts[1], L. J. Kecskes[3],
R. Rowland[2], S. P. Mates[1] and S. D. Ridder[1]

[1]NIST, 100 Bureau Drive, STOP 8556; Gaithersburg, MD 20899-8556
[2]MATSYS, Inc., 504 Shaw Road Suite 215, Sterling, VA 20166
[3]US ARL, Aberdeen Proving Ground, MD 21005-5069

Keywords: Amorphous metal powder, HIP consolidation, Material properties

Abstract

Amorphous metal alloys have been developed with sufficiently slow crystallization kinetics to allow the casting of bulk metallic glass (BMG) components up to several centimeters in cross section. Mechanical characterization of these castings has shown that these new BMG alloys have high modulus, high elastic limits and high hardness, as compared to crystalline metal alloys. The extension of this technology to the production of large structural amorphous metal components will require the consolidation of amorphous particles. NIST, MATSYS, and ARL are studying the response of several amorphous metal alloys to HIP consolidation. This paper will present the results of these studies on consolidated monolithic BMG alloys and tungsten-BMG composites. Recent results on the HIP consolidation mechanics and the resultant microstructures of the samples are discussed.

Introduction

Bulk metallic glasses (BMG) are a relatively new class of metallic alloys. They possess high yield strength, high moduli, high hardness and elastic-strains exceeding 2 %. Generally these alloys are found at or near deep eutectics, have high viscosity in the melt, and contain three or more constituents. A small element atom and a large element atom are frequently added to further slow down the kinetics [1] and thus allow the high viscosity liquid to freeze without crystallization occurring [2-6]. The amorphous solid formed has unique mechanical, corrosion and physical properties [2-5, 7]. The easiest forming BMG alloy is $Zr_{41.2}Ti_{13.8}Cu_{12.5}Ni_{10}Be_{22.5}$ with a critical cooling rate of 1 Ks^{-1} [2, 3]. This alloy has been cast in sizes up to 100 mm in diameter. However, this size BMG ingot is unique to this composition only. In general, these BMG alloys can only be cast in ingots a few centimeters or less in diameter and a few millimeters in thickness.

The challenge is to develop a process to produce large monolithic and composite structures from BMG alloys, e.g., tungsten heavy alloy composites. Only one BMG alloy has been cast up to 100 mm in diameter [8] and this alloy is not acceptable for most applications because it contains beryllium, an element toxic to many individuals. One approach for creating large-scale BMG components would be to produce gas-atomized, amorphous powders and then consolidate these powders into structural amorphous materials by Vacuum Hot Pressing (VHP), Warm Isostatic Pressing (WIP), Hot Isostatic Pressing (HIP), hot extrusion or a combination of these processes. Ideally, the processing route will avoid the liquid state and preserve the original amorphous structure of the powder. Researchers at the Ames Research Laboratory consolidated a gas-atomized $Cu_{47}Ti_{34}Zr_{11}Ni_8$ amorphous powder by warm extrusion with some success [7].

A processing window of opportunity exists in BMGs in the temperature interval (ΔT) between the glass transition temperature (T_g) and the first crystallization temperature (T_x). The width of this temperature window ($\Delta T=T_x - T_g$), in combination with the reduced glass transition temperature ($T_r = T_g / T_l$; where T_l is the liquidus temperature), define the glass forming ability (GFA) of the alloy. The amorphous powder can be heated in the super cooled liquid state (in the ΔT region) for some time without crystallization occurring. Some of the more recently identified BMG alloys [9] have a wide temperature window. A consolidation process can be developed to take even further advantage of this processing window and prevent even partial crystallization.

The consolidation process chosen for this work is HIP. Our approach is to use an instrumented-HIP to monitor the densification of the amorphous powders during the HIP cycle. The HIP schedule can be adjusted in real time to control the exposure of the amorphous powder to maximum temperature and the time required at maximum temperature to achieve full densification. As a result, the microstructure of the starting powder is preserved, and compacts of high amorphous content are expected.

At the onset of this study a ready supply of amorphous powders was not available. In order to test the feasibility of producing large components by consolidating gas-atomized, amorphous powders via instrumented-HIP consolidation, it was decided to take advantage of the readily available powders produced at the INEEL [10]. Although many of these powders are not fully amorphous it was felt some of them would be adequate for this feasibility study.

Instrumented-HIP Equipment

An instrumented-HIP is used for consolidation of amorphous powder specimens. The HIP can be operated up to 200 MPa (29 ksi) pressure and 1400 °C. The sensor used for monitoring consolidation is a High Temperature Eddy Current Sensor (HiTECS). HiTECS is based on the principle of eddy current sensing which is a combination of two effects, electromagnetic and magneto-electric [11]. These effects are controlled and measured respectively to achieve shape change and property measurements of electrically conductive materials in close proximity to the sensor's coils. The global sensor design used to measure cylindrical specimens consists of loose wound concentric platinum coils around cylindrical boron nitride insulators. The outer "drive coil" is swept with a broadband signal, which is inductively coupled to a second platinum inner coil known as the "pickup coil". Wide shallow grooves allow the coil wire to expand and contract under thermal loading along the sensor's axial dimension while constraining its radial movement. This simple design maintains a constant fill factor (relative radial position) between the drive and pickup coils, providing an integral mechanical-thermal compensation of the sensor's response. The sensor's response to conductive materials is affected by a change in the mutual inductance of the coils. A two-coil transfer impedance can be measured by $Z_m = V_p / I_d$, where V_p is the voltage across the pickup coil and I_d is the current in the driver coil, as illustrated in Figure 1. The complex impedance plane for a broad frequency span yields characteristic curves, as illustrated in Figure 2. Measurements of geometrical changes that occur to the specimen requires application of the eddy current "skin effect" given by:

$$\delta = \left(\pi f \mu \sigma\right)^{-1/2} \tag{1}$$

where,

δ = skin depth,

f = frequency of the driving current,

μ = permeability, and

σ = conductivity of specimen.

The sensor exciting frequency range is tuned for the conductivity of the specimen material so that the penetrating depth of eddy currents can be selected. If the desired result is specimen dimensional change, high frequencies below the knee of the characteristic impedance curve are used. On the other hand, if sub-surface microstructural changes are desired, low frequencies above the knee of the characteristic impedance curve are used. As an example of this response, characteristic impedance curves are illustrated in Figure 2 for four changes in sensor/specimen proximity, which result from scanning the specimen with a broad frequency sweep (2 kHz to 800 kHz). The measurement is normalized to the sensor response with no specimen present. As the high frequency points move up the imaginary axis the specimen is consolidating, i.e. moving away from the inside diameter of the sensor. Using a set of standards (precisely machined diameter tubes) a sensitivity equation is determined to convert imaginary intercept into diameter change. Using initial relative density and conservation of mass principle, the diameter measured is translated into relative density measurement of the material.

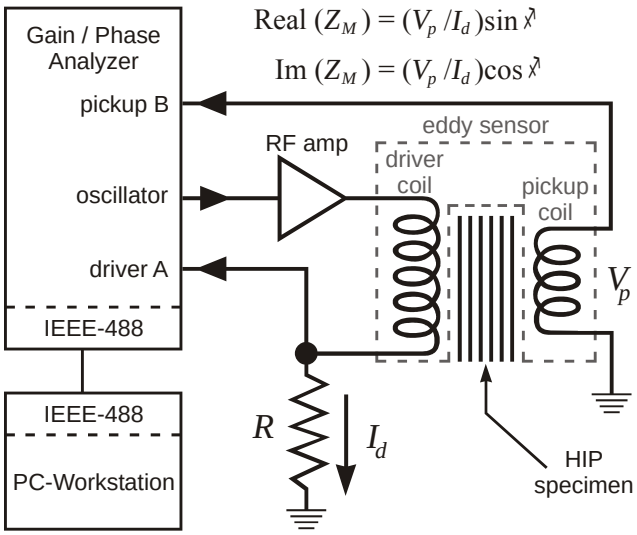

Figure 1: HiTECS sensor schematic.

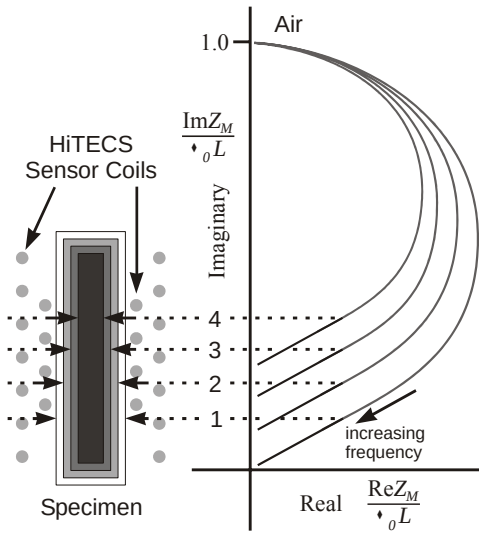

Figure 2: Characteristic complex impedance curves.

Subsequent to HIP operations, representative samples were cut from the consolidated specimens for metallography, Vickers microhardness, X-ray Diffraction (XRD), optical and Scanning Electron Microscopy (SEM) analyses. Fracture surfaces were obtained by impact loading the as-cut samples with a hammer. Additionally, differential thermal analysis (DTA) was performed on the as-received "DAR 27" iron-based amorphous powder from INEEL (Idaho Falls, ID) [10].

Results and Discussions

Characteristics of the Iron-Based "DAR27" and Ultrafine Tungsten Precursor Powders

The amorphous iron material, "DAR27," is a multicomponent iron-based metallic glass received from INEEL [10]. It consists of generally spherical particles ranging in size from 2 μm to 15 μm. As shown in Figure 3, the as-received powder is essentially X-ray amorphous (Figure 3a). It exhibits a glass transition temperature at 560 °C and a single crystallization temperature at 590 °C, indicative of a rather narrow undercooled region. Note that the wide temperature gap between its solidus and liquidus, at 1110 °C and 1320 °C, respectively, is strongly reflective of the complexity of its structure and melting behavior. The tungsten powder, used in this effort, was an off-the-self stock item P30-3, obtained from

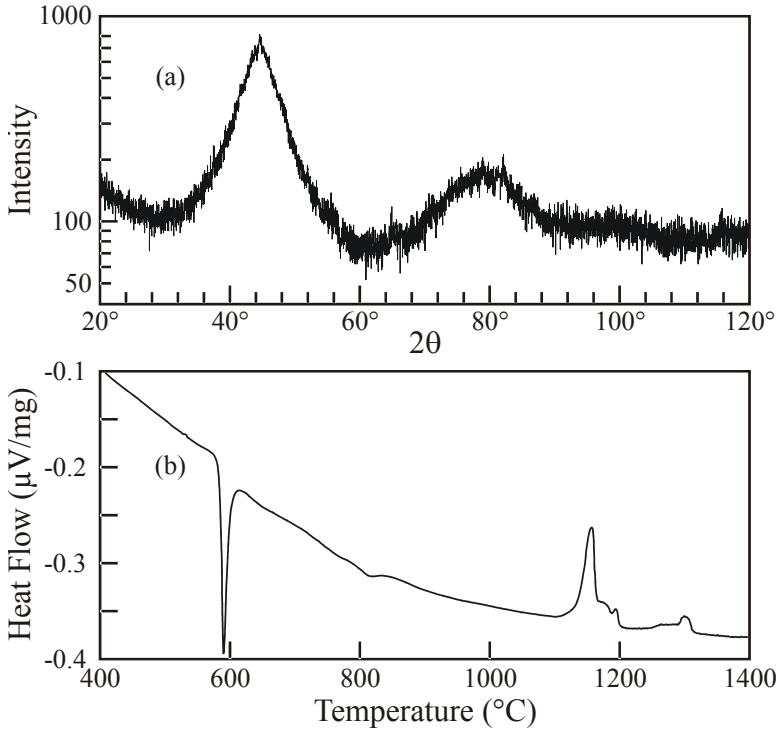

Figure 3: An X-ray diffractogram in (a) and a DTA thermogram in (b) of the as-received iron-based amorphous powder.

Alldyne Corporation (Huntsville, AL)[12]. Nominally, it is a sub-micrometer powder that agglomerates into 20 μm to 40 μm aggregates.

Consolidation of Monolithic Material

An instrumented-HIP experiment was performed on a HIP canister with a diameter of 25.4 mm (1 in) and length of 140 mm (5.5 in). The canister was filled with the iron-based amorphous powder, "DAR27," received from INEEL [10]. To estimate the initial powder packing (fill) density, dimensional and weight measurements were conducted on the empty and full canister. The canister was then evacuated and e-beam welded. The HIP canister was inserted inside the sensor and the diameter was monitored. The HIP schedule used for this experiment is illustrated in Figure 4a where pressure and temperature measurements taken during the HIP run are shown. The corresponding HIP canister diameter change measured by HiTECS is illustrated in Figure 4b. The HIP temperature was initially held at 100 °C while the pressure was ramped to 100 MPa (14.5 ksi). Subsequently, both temperature and pressure were increased simultaneously, until densification was observed. Subsequently, the temperature was held constant for 15 min but no further densification was observed. The experiment was stopped and the specimen was removed for characterization.

The measurement illustrates two unique features in the densification behavior of this amorphous powder. The first feature is the very high densification rate once a critical temperature is reached. This temperature window is near the crystallization temperature (T_x) of this amorphous powder. This behavior has not been observed on crystalline metals and ceramic powders. The second feature is the abrupt stop in densification at 640 °C. Typically for crystalline alloys, the densification rate decreases as the material approaches full density unlike the behavior displayed by this amorphous powder.

To verify this unique behavior, a second HIP canister was prepared and consolidated under the same conditions. The same unique behavior was observed again. This time since the specimen had not reached full density, the temperature was further increased to identify the temperature at which full

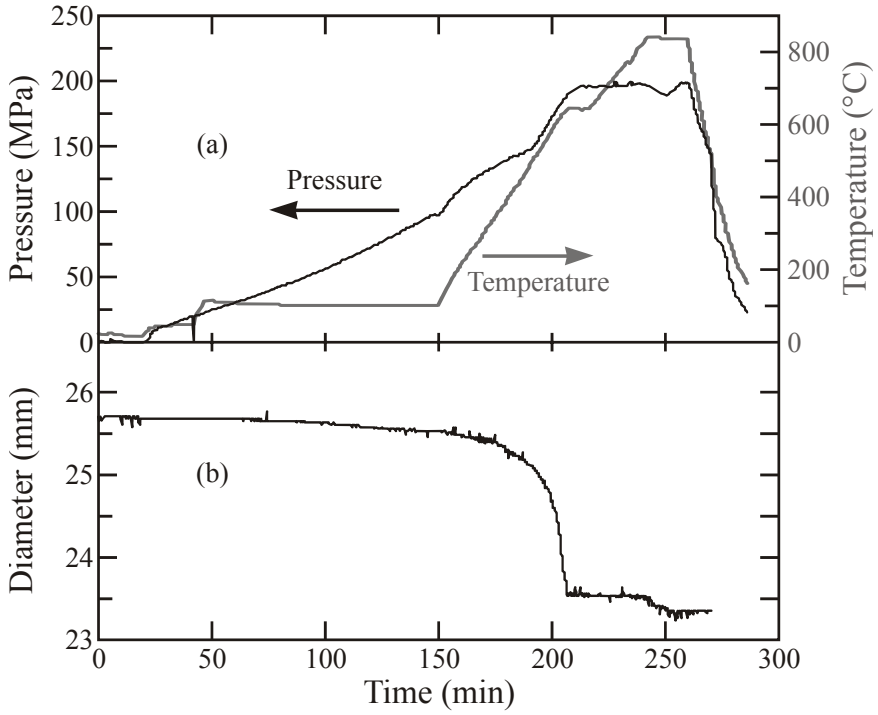

Figure 4: HIP schedule in (a) and densification behavior in (b) for iron-based amorphous powder.

densification may occur. Further densification occurred at 850 °C. Subsequently, the temperature was held constant for 30 min and then the HIP was vented and cooled to room temperature.

Metallographic image analysis was used to measure the density and Vickers hardness of the HIP-consolidated specimens. The specimens consolidated at 640 °C had a Relative Density (RD) = (94.0 ±0.8) % and a Vickers hardness = (980 ±170) HV 1 [13] as shown in Figures 5a and 6a respectively. The specimens consolidated at 850 °C had a RD = (99.6 ±0.8) % and a Vickers hardness = (1242 ±70) HV 1 as shown in Figures 5b and 6b respectively. The measured hardness is in the range reported by INEEL for this class of material.

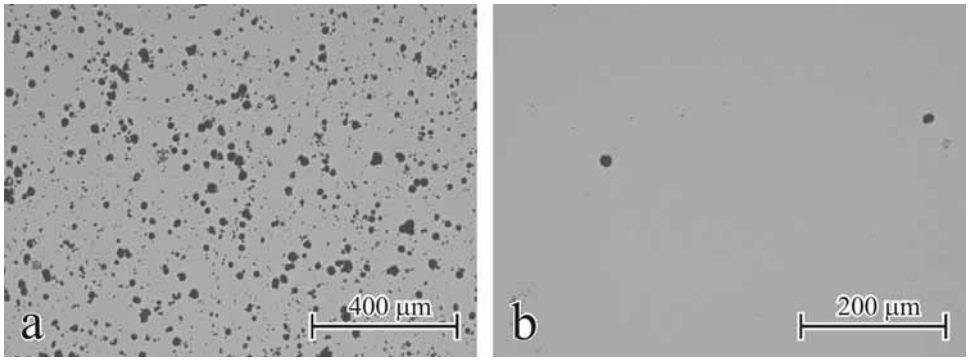

Figure 5: Metallographic porosity measurements of HIP-consolidated iron-based amorphous powder.
a) HIP temperature = 640 °C, RD = (94.0 ±0.8) % by image analysis.
b) HIP temperature = 850 °C, RD = (99.6 ±0.8) %.

Closer examination by SEM of polished (Figures 7a) and fracture surfaces (Figures 7b) of the HIP-consolidated iron-based amorphous powder reveals that, at 640 °C the sample consists of a homogeneous structure of partially deformed spheroidal particles with porosity residing in the triple points between particles. Furthermore, bonding is relatively poor as evidenced by the intergranular failure between particles or 'grains.' In contrast, the SEM micrographs of the polished cross sectional

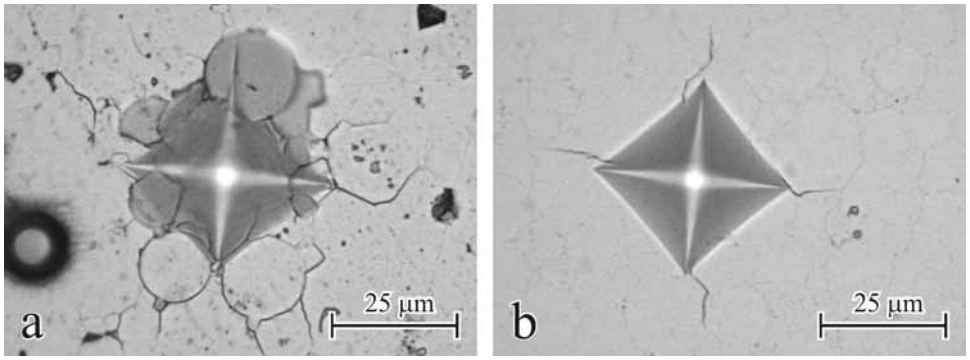

Figure 6: Metallographic hardness measurements of HIP-consolidated iron-based amorphous powder.
a) HIP temperature = 640 °C, Vickers hardness = (980 ±170) HV 1.
b) HIP temperature = 850 °C, Vickers hardness = (1242 ±70) HV 1.

and fracture surfaces (Figures 8a and 8b) demonstrate a significant improvement in consolidation and bonding at 850 °C. The aforementioned porosity is absent and there is a large number of grains that failed by transgranular fracture. However, an added consequence of processing above the recrystallization temperature is the apparent devitrification of the amorphous structure. XRD of the consolidated samples confirmed the decomposition of the amorphous alloy and evolution of a nanostructured product. Energy dispersive analysis of the lighter second phase, shown in Figure 8c, indicates it is rich in tungsten, iron, and chromium.

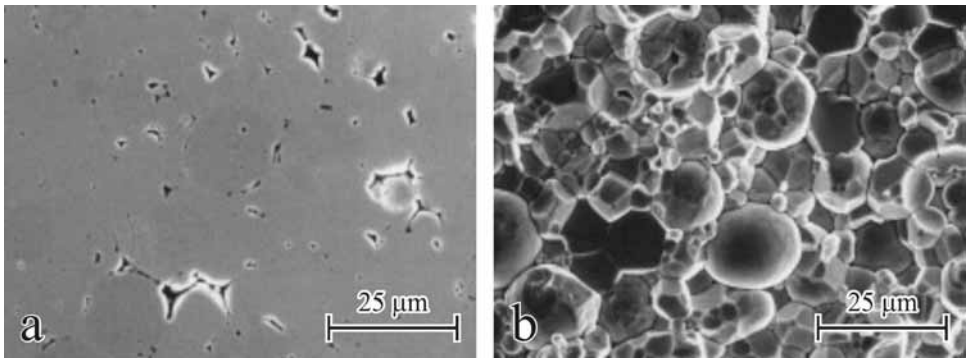

Figure 7: SEM micrographs of polished (a) and fracture surfaces (b) from the monolithic material processed with a HIP temperature = 640 °C.

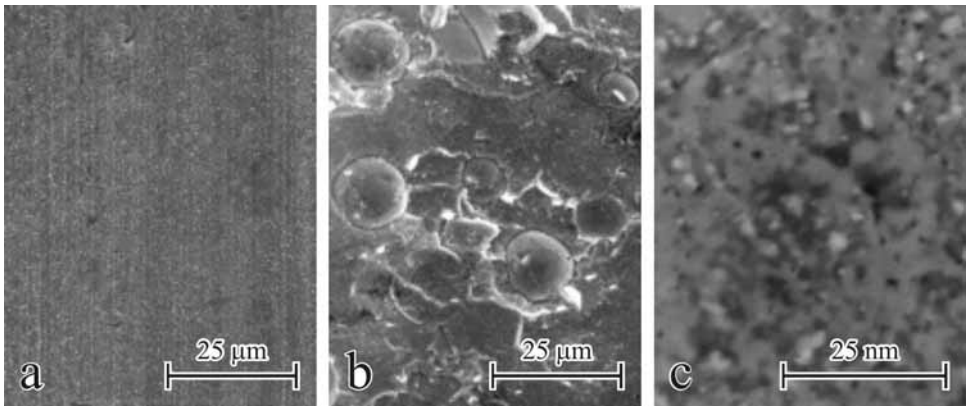

Figure 8: SEM micrographs of the monolithic material processed with a HIP temperature = 850 °C. Polished cross section is shown in (a), fracture surface in (b), and partially devitrified structure in (c).

Observations

Most of the consolidation of the powder occurred below or near the crystallization temperature, as expected. Full densification could not be reached for this material within the processing window that would allow the material to remain fully amorphous. We believe that despite the amorphous nature of the starting powder, the narrow undercooled region limits the ability to obtain fully dense amorphous bulk material. That is, during processing, near or below the crystallization temperature, little or no deformation and flow occurs, however, nucleation of nanocrystals initiates rapidly. Most likely, the appearance of this fine structure impedes flow and deformation, which, in turn, requires a temperature higher than the crystallization temperature to consolidate. However, once devitrified, the crystallized, nanostructured material is considerably harder and stronger. As such, further experiments need to be performed on this amorphous powder.

Consolidation of Composite Material

A blend of 80 % tungsten powder and 20 % amorphous iron powder (volume %) was then prepared and HIP canisters were filled, evacuated and sealed. Again, instrumented-HIP experiments were then performed on tungsten-amorphous powder composites. Two experiments have been completed. The composite was HIP-consolidated at 850 °C maximum temperature in the first experiment and at 1161 °C maximum temperature in the second experiment.

Metallographic image analysis of the composite material consolidated at 850 °C indicated a relative density = (74.0 ±0.8) % and a Vickers hardness = (197 ±37) HV 1 as shown in Figures 9a and 10a

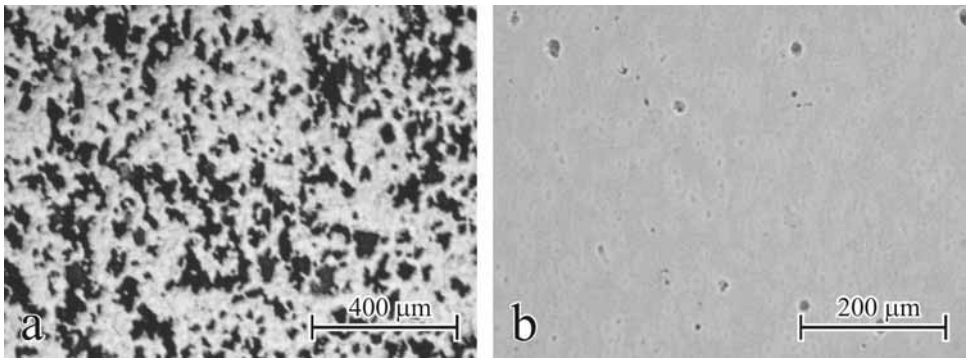

Figure 9: Metallographic porosity measurement of HIP-consolidated composite material.
a) HIP temperature = 850 °C, RD = (74.0 ±0.8) %.
b) HIP temperature = 1161 °C, RD = (99.0 ±0.8) %.

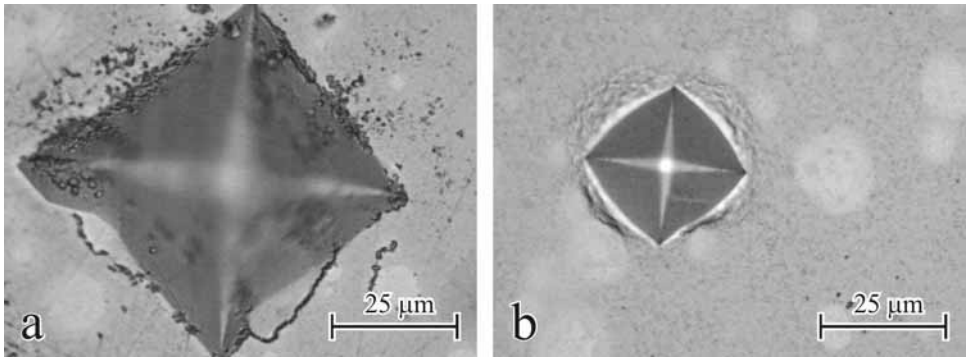

Figure 10: Metallographic hardness measurement of HIP-consolidated composite material.
a) HIP temperature = 850 °C, Vickers hardness = (197 ±37) HV 0.5.
b) HIP temperature = 1161 °C, Vickers hardness = (1023 ±66) HV 0.5.

respectively. Consolidation at 1161 °C produced a relative density = (99.0 ±0.8) % and a Vickers hardness = (1023 ±66) HV 1 as shown in Figures 9b and 10b respectively. The composite material processed at 1161 °C appeared to display localized shear band failure around the hardness indent in Figure 10b, which is a desirable feature for the target application [14].

Examination of the HIP-consolidated composite materials indicated a good dispersion of the iron-based BMG with tungsten. At 850 °C, as the SEM micrographs depict in Figure 11, the BMG particles are uniformly dispersed in the tungsten phase. However, intergranular fracture, primarily occurring in the tungsten phase, dictates the overall failure of the composite. Moreover, as evidenced in the fracture surface image, failure of the BMG particles does not occur, as they simply pull out of the tungsten phase. As shown in Figure 11c, the iron-based amorphous particles readily devitrify at this temperature. At the same time, note the poor consolidation quality of the tungsten phase with extensive, uniformly dispersed porosity in between the grains. Again, XRD verified the decomposition of the amorphous structure.

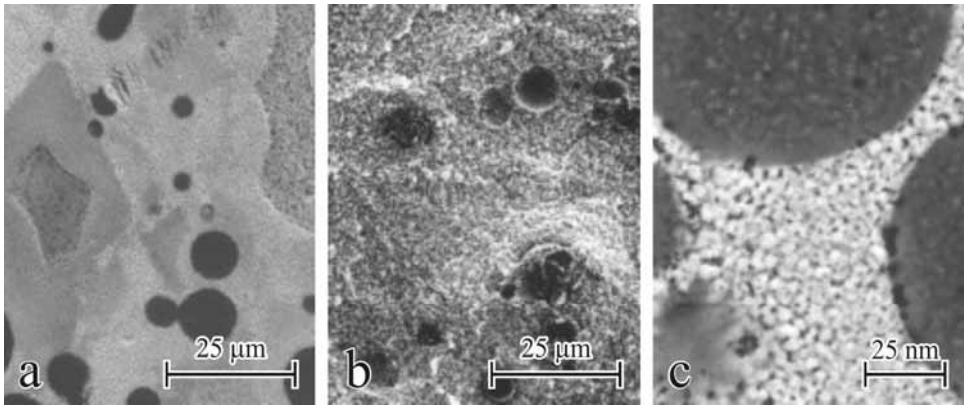

Figure 11: SEM micrographs of consolidated composite material processed with a HIP temperature = 850 °C. Polished cross section is shown in (a), fracture surface in (b), and close-up of (a) in (c) showing devitrification of the BMG powder and poor intergrain bonding of the tungsten phase.

The quality of bonding of the two phases considerably increases at 1161 °C. As shown in Figure 12, a strong interfacial reaction layer, forming between the BMG particles and the adjacent tungsten phase, imparts some strength to the composite. The intermediate layer consists of tungsten-iron intermetallics. Nevertheless, the weakness of the tungsten phase still dominates the fracture of the composite material. It should also be noted that despite the apparent intergranular structure shown in Figure 12, the Vickers hardness measurements were constant across both phases within this material.

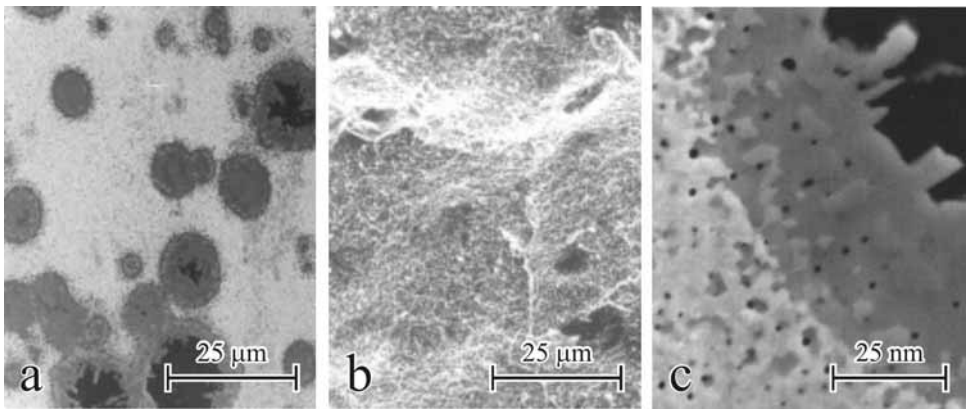

Figure 12: SEM micrographs of HIP-consolidated composite material at 1161 °C. Polished cross section in (a), fracture surface in (b), and close-up of (a) in (c) showing devitrification of the BMG powder and tungsten-iron intermetallic interfacial reaction layer.

Observations

Consolidation of the composite material required higher temperatures than the monolithic BMG material. Results at the lower processing temperature did not allow adequate bonding to occur between the two phases. In contrast, treatment, near the solidus of the BMG, greatly improved consolidation quality. The composite also developed a crystallized fine structure as a consequence of the higher temperature treatment, wherein the devitrified BMG particles reacted with the tungsten phase to form an interfacial layer improving bonding. However, despite the improvement in bonding, the inherent weakness of the tungsten phase limited the usefulness of the composite product. It is believed that further improvements to the tungsten phase, such as reducing impurity levels or adjusting the particle and/or grain size, will enhance the performance of the composites [14].

Summary and Conclusions

Instrumented-HIP runs have been conducted to monitor and develop a process for consolidation of amorphous powders into bulk amorphous materials. The results identified the temperature window in which consolidation occurs. Two unique features about the densification of amorphous powder have been observed, namely, very high densification rate and abrupt stop of densification. These features can be exploited to achieve the goal of larger scale production of BMG powder-based bulk amorphous composite materials. However, the starting materials need to be more compatible. For HIP to be effective, better matched starting sizes, higher starting purities, and a wider processing window will be necessary. Efforts are underway to acquire higher purity tungsten precursors as well as to atomize BMGs with better glass forming ability.

Acknowledgements

The authors wish to thank P. A. Boyer, D. I. Wickner, and R. H. Woodman for their assistance with the processing and characterization, and C. Handwerker for valuable discussions. The authors also wish to acknowledge support from DARPA, ONR, and NIST.

References

1. O.N. Senkov and D.B. Miracle, "Effect of the Atomic Size Distribution on Glass Forming Ability of Amorphous Metallic Alloys," *MRS Bulletin* 36 (2001), 2183-2198.

2. W.L. Johnson, "Bulk Glass-Forming Metallic Alloys: Science and Technology," MRS Bulletin, Oct. 1999, 42-56.

3. S.C. Glade et al., "Thermodynamics of $Cu_{47}Ti_{34}Zr_{11}Ni_8$, $Zr_{52.5}Cu_{19.7}Ni_{14.6}Al_{10}Ti_5$ and $Zr_{57}Cu_{15.4}Ni_{12.6}Al_{10}Nb_5$ Bulk Metallic Glass Forming Alloys," *Journal of Applied Physics*, 87 (10) (2000), 7242-7248.

4. Y. Li, "A Relationship between Glass-Forming Ability and Reduced Glass Temperature near Eutectic Composition," *Materials Transactions*, 42 (4) (2001), 556-561.

5. J.M. Pelletier, J. Perez, and J.L Soubeyroux, "Physical Properties of Bulk Amorphous Glasses: Influence of Physical Aging and Onset of Crystallization," *Journal of Non-Crystalline Solids*, 274 (2000), 301-306.

6. W.J. Boettinger et al., "Eutectic Solidification and the Formation of Metallic Glasses," *Rapid Solidification Processing*, R. Mehrabian, B.H. Kear, and M. Cohen Eds. (Claitor's Publishing Div., 1980), 50-55.

7. D.J. Sordelet et al., "Synthesis of $Cu_{47}Ti_{34}Zr_{11}Ni_8$ Bulk Metallic Glass by Warm Extrusion of Gas Atomized Powders," *J. Mater. Res.*, 17 (1) (2002), 186-198.

8. R.B. Dandliker, R.D. Conner, and W.L. Johnson, "Melt Infiltration Casting of Bulk Metallic-Glass Matrix Composites," *J. Mater. Res.*, 13 (10) (1998), 2896-2901.

9. R.E. Hackenberg et al., "Thermodynamics and Phase Equilibria of the Al-Fe-Gd Metallic Glass-Forming System," *Acta Materialia*, 50 (2002), 2245-2258.

10. D.J. Branagan, Private communication with author, INEEL, 2002.

11. H.N.G. Wadley et al., "Sensing and Modeling of Hot Isostatic Pressing of Copper Powder," *Hot Isostatic Pressing: Theory and Applications*, R.J. Schaefer and M. Linzer Eds. (ASM International, 1989), 91-99.

12. The use of commercial products or trade names is for identification purposes only. Such identification is not intended to imply endorsement or evaluation of the relative merits of these items by the National Institute of Standards and Technology.

13. Vickers hardness values are shown in the format preferred by ISO as *x* HV *y*, where *x* is the measured value in kg-force/mm^2 (x·9.80665 MPa) and *y* is the mass in kg used to load the indenter. The expanded uncertainties shown for the density and hardness measurements = 2σ.

14. F.S. Biancaniello et al., "Characterization of Nanostructured Tungsten Heavy Alloy Produced by Double Ball Milling," *Tungsten Refractory Metals and Alloys 4*, A. Bose and R.J. Dowding Eds. (MPIF, 1998), 213-218.